HEFAT2014
10th International Conference on Heat Transfer, Fluid Mechanics and Thermodynamics
14 – 16 July 2014
Orlando, Florida

CONVECTIVE HEAT TRANSFER IN CELLULAR CERAMIC: A 3D NUMERICAL SOLUTION

L. Ferrari, M.C. Barbato*, A. Ortona, C. D'Angelo
*Author for correspondence
University of Applied Sciences of Southern Switzerland,
DTI – Department of Innovative Technologies
Manno, 6928,
Switzerland
E-mail: maurizio.barbato@supsi.ch

ABSTRACT

In this work, three-dimensional thermo fluid dynamics analyses were performed in order to evaluate the convective heat transfer coefficient for cellular ceramics, both random (i.e. foams) and regular (i.e. lattices). The study aimed at evaluating the heat exchange performance of cellular ceramics with the scope of engineering their morphology in order to maximize the ratio between heat exchange and pressure drop.
Performed simulations focus on capturing the relevance of cell morphology on thermal convection and pressure drop of cellular ceramics within a porosity range of 75–90% and at different fluid velocities. Computational analyses were performed with the commercial CFD package ANSYS-Fluent. Results show that parameters affecting most the pressure drop are porosity and cell aspect ratio; on the other hand, the thermal convective coefficient is strongly dependent on surface area, which, in turn, is directly related to cell morphology.

NOMENCLATURE

m	[kg/s]	Mass flow rate
Ds	[mm]	Strut diameter
Ls	[mm]	Strut length
H	[mm]	Cell height
L	[mm]	Foam or lattice length
D_h	[mm]	Foam or lattice hydraulic diameter
p	[Pa]	Static pressure
Δp	[Pa]	Pressure drop
T	[K]	Temperature
ΔT	[K]	Difference of temperature
Nu	[-]	Nusselt number
Pr	[-]	Prandtl number
Re	[-]	Reynolds number
Re_p	[-]	Pore Reynolds number
U	[m/s]	Velocity
V	[mm^3]	Volume

Special characters

μ	[Pa s]	Dynamic viscosity
ρ	[kg/m^3]	Mass Density
ε	[-]	Porosity

Subscripts

wall	Wall foam/lattice
inlet	Inlet of the computational domain
outlet	Outlet of the computational domain
pore	Pore of the foam or lattice

INTRODUCTION

Cellular ceramics are a specific class of porous materials which consists in three-dimensional arrangements of periodic cells. Cells' morphology may be random in the case of foams or repeatable for lattices. Foams are nowadays widely used for high temperature applications such as molten metals filtering, catalytic supports, porous burners or radiation absorbers in solar plants [1]. Their high specific area, high temperature resistance and low weight make them a matchless material for the above mentioned applications, especially where heat transfer and high temperatures are considerable. Among the future high temperature applications of ceramic cellular structures, Thermal Protection Systems (TPS) for space re-entry vehicles is one of the most promising. These vehicles, when re-entering a planetary atmosphere, are exposed, for a short period of time, to extreme thermal loads. These operative conditions bring to very high temperatures and cause thermal shocks to structural components. These loads can be partially reduced with the use of an active cooling system where a fluid is flown through high temperature resistant cellular structures, namely SiC based cellular ceramics.
Reticulated porous materials have been widely used as heat exchangers in the last years because of their outstanding behavior when convective heat transfer is concerned. The effect

of tetrakaidecahedra lattices morphological features such as: cell inclination, ligament tapering and ligament radius was analyzed in a previous paper [4].
Zhiyong Wu [5] investigated the convective heat transfer by varying average cell size and number. In the literature, when analyzing ceramic foams, their performance is usually shown in terms of pressure drop vs cell size and porosity.

Very often these materials present narrow property ranges because they are produced by foaming of a polymeric template followed by replica [2], both processes are difficult to control. With the aim of controlling their performance, the production process allows acting on few parameters, such as cell size (while foaming) and struts thickness (while replicating). For foams, the first parameters can be controlled on average, being cell size and shape randomly placed in the space. A solution to have more control to the cellular materials morphology was solved [3] with a method based on 3D printing of polymeric lattices which, designed with specific characteristics, were successively converted into cellular ceramics via replica.

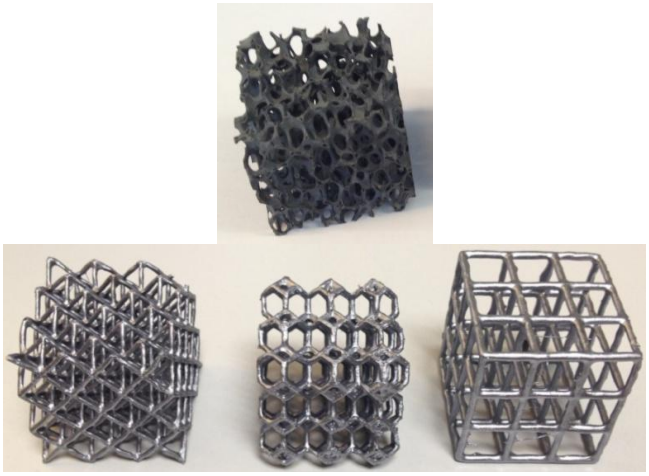

Figure 1 Real foam and real lattices morphologies

The morphology of random foams makes them behave as isotropic materials. Occasionally, some applications need porous media with anisotropic and repeatable features. With the new approach of [3], lattices with specific performance tailored and designed by CFD simulations, can be realized.
In this work, thanks to CFD, it was possible to study heat transfer performance, namely pressure drop and convective heat transfer, for both foams and lattices as a function of their porosity.

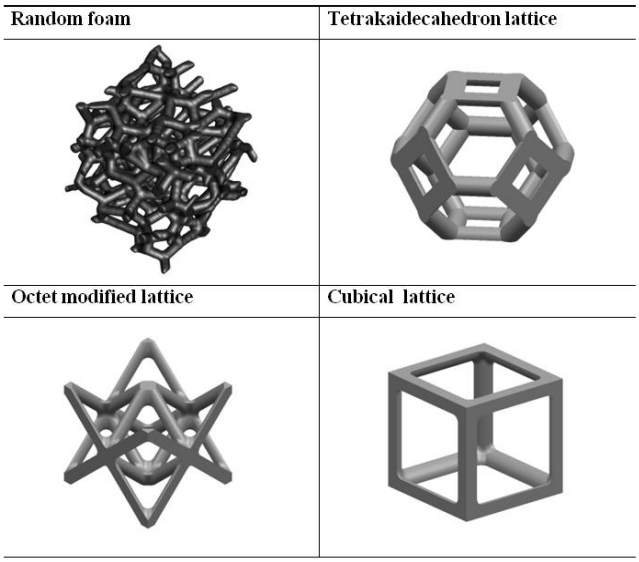

Figure 2 Foam and lattices morphologies

Table 1: Foam and lattices parameters

	Ls [mm]	Ds [mm]	ε [-]	Connectivity [-]
Random Foam	5	3	0.8	4
Tetrakaidecahedron	3.54	2.2 2 1.3	0.75 0.8 0.9	4
Octet modified	7.07	1.8 1.62 1.12	0.75 0.8 0.9	8
Cubical	10	3.7 3.2 2.2	0.75 0.8 0.9	6

NUMERICAL MODELING

The definition of the computational domain (CD) and the computational mesh construction was done with two different approaches for random foams and for lattices. They are presented in the following.

Computational Domain Construction for Foams

For the random foam, in order to control foam topologic parameters, an artificial foam generation was performed. This procedure consisted in the reverse engineering of a real foam passing through image acquisition via TAC, image treatment via a dedicated sw (AVIZO [6]) and then 3D solid object reconstruction via CAD.
The virtual foam was slightly modified in order to obtain cylindrical struts, which in reality have a cross section with tricuspid shape. This was done to decouple the morphology

effects from those due to the strut shape. The latter were in fact studied in a previous paper [6,7]. Therefore the 5 PPI foam was then described by three fundamental parameters as done for lattices: strut length, diameter and connectivity.

The CD was then obtained by Boolean subtraction of the solid reconstructed foam from another homogeneous solid representing the volume of fluid. Figure 4 shows the complete computational domain for the random foam. Notice that two additional volumes of fluid were added in front and behind the lattice: the former allows the fluid flow to smoothly approach the solid, the latter is placed to avoid reverse flow at the outlet.

Computational Domain Construction for Lattices

The three typologies of lattices analyzed in this paper are all matrixes, composed of three identical base cells each one occupies a volume of 10x10x10 mm^3. These three base cells are: cube, octet modified and tetrakaidecahedron (TetraK). The modified octet was obtained by simplifying the regular-octet in order to obtain an extremely anisotropic base cell. The tetrakaidecahedron was chosen because it is the structure that better approximates random foams. Finally, the cube was selected so as to have a reference case of the simplest geometry.
As done for the foams, lattices are characterized by three fundamental quantities: strut length, diameter and connectivity. Likewise important is the porosity, which is directly related to the strut diameter, and is defined as:

$$\varepsilon = V_{pore}/V_{total} \qquad (1)$$

It is important noting that parameters reported in Table 1 are mean values.

The computational domain creation for lattice structures required less effort with respect to foams. Three lattice cells, aligned in the flow direction, were designed via CAD, then, a Boolean subtraction of the solid lattice to the volume of fluid produced the computational domain at once.
The lattices complete computational domain can be seen in Fig. 5.

Mesh generation

Foams and lattice computational domains were meshed with two different software ANSYS-WorkBench [7] and HyperMesh-HyperWorks [8], but the same meshing strategy was applied. In fact, the mesh consists of two regions: a boundary layer region attached to the solid surface realized extruding an unstructured triangular surface mesh and a unstructured tetrahedral mesh in the bulk. The boundary layer extrusion height was limited to a maximum of 0.2 mm to avoid an excessive cells distortion occurring in the case of random foams. Figure 3 reports a section of the computational domain were the mesh topology is shown.

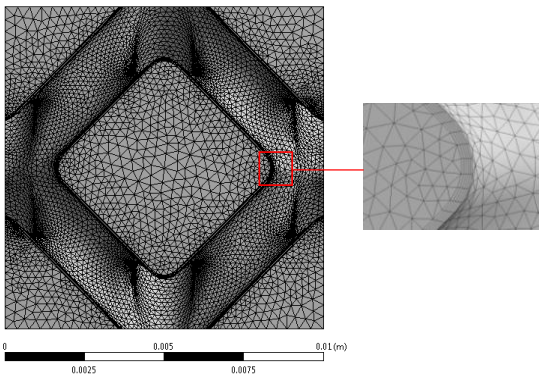

Figure 3 An example of the CFD mesh used in the present work

Modeling equations

The Computational Fluid Dynamics approach assumes an uncompressible, steady, three dimensional flow. Navier-Stokes, mass conservation, and energy equations were solved with a pressure-based approach [9]. Radiative heat transfer is not accounted for in the energy equation because the solid surface temperature is uniform and air is an optically thin fluid. Constant values were assumed for thermal and transport properties thanks to the very small temperature variations involved in the flow. Mass density was calculated with the ideal gas equation.
The Reynolds number calculation was based on the "pore Reynolds number approach" suggested by Gibson, Ashby [10, 11]

$$Re_p = \frac{\rho \cdot U_{inlet} \cdot D_h}{\mu} \qquad (2)$$

with the laminar-turbulent flow transition limit set at Re_p=150. The turbulence model applied, as a consequence of the flow regime detected, is specified in the following section.

Turbulence model
The steady state turbulent flow was solved with RANS approach. A preliminary screening with four different turbulence models, k-ε standard, k-ε Realizable, k-ε RNG, and k-ω SST was performed. No major differences were found in the behavior of k-ε models. Based on the Reynolds number values and considering the tortuosity of the flow, the k-ε Realizable was chosen.

Boundary Conditions

Figures 4 and 5 show the boundary conditions imposed to the computational domain. At the flow inlet a constant velocity was imposed with values ranging from 1 to 6 m/s. The air inlet temperature was set at 300 K for all tests. At the outlet a constant relative pressure boundary condition was imposed. For the lattice cases the lateral walls of the CD were set as symmetry boundaries. For the random foam (Figure 4) the external faces were set as adiabatic solid walls. This because, in this case, the CD cross-section is larger than that of a lattice single cell; furthermore, it was not possible to exploit symmetry or periodicity. To eliminate possible edge effects and coherently compare the flow behavior for lattice and random foams, results for the latter were gathered from a smaller inner channel far from the adiabatic walls as shown in Figure 6. The inner channel cross section has the same dimensions of that of the lattice channel, i.e., 10x10 mm^2.
The boundary condition for the energy equation at the lattice and random foam solid surfaces was set to uniform and constant temperature with the value set to 330 K.

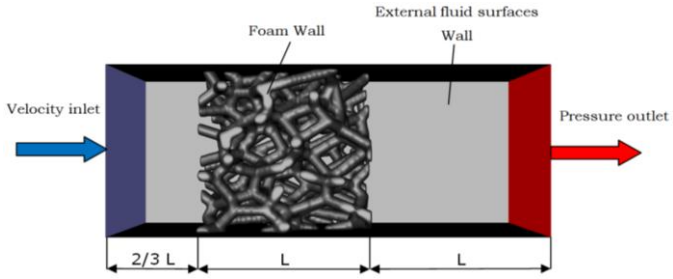

Figure 4 The computational domain and boundary conditions of the random foam

For the turbulence model, the Enhanced-Wall-Treatment was used. This is a weighted blend of standard wall function and accurate boundary layer resolution based on the y^+ value [7].

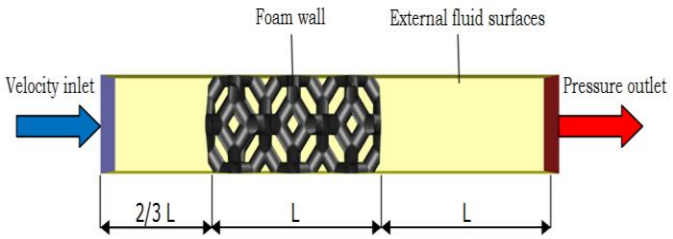

Figure 5 The computational domain and boundary conditions of the lattices

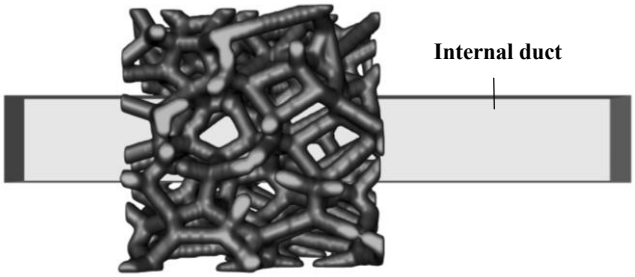

Figure 6 Internal channel in random foam

Numerical methods

The fluid flow equations are solved with a Finite Volume Method by using the commercial software ANSYS-Fluent.
A Second Order Upwind numerical scheme [9], was used for mass, momentum, temperature, and turbulence model equations.
Convergence of the iterative process was monitored with two conditions that must be simultaneously satisfied:

- Discretized equations residuals must be below the following values: 10^{-3} for momentum, 10^{-4} for continuity, k and ε, 10^{-6} for energy.
- Variations of the average temperature at the outlet must be below 10^{-2} K.

RESULTS DISCUSSION

Pressure drop evaluation

When talking about internal flow, pumping power can become an issue. The pumping power is directly proportional to the flow pressure drop. The latter, therefore, plays a fundamental role in the evaluation of porous media performance. In this work it is calculated as:

$$\Delta p = p_{inlet} - p_{outlet} \quad (3)$$

Form the boundary conditions imposed, at outlet the static pressure is always zero, therefore, the pressure drop through the porous media corresponds to the pressure value measured at the inlet section. The inlet pressure value was calculated as an area average over the inlet section. All samples numerically tested had the same length, therefore pressure drop values were compared directly and were not scaled with sample length. Results of pressure drop are shown by Figure 7. For all porous morphologies studied, pressure drop coherently increases with air velocity. The random foam performance is outstanding with respect to porous media with same porosity. Better performance are offered only by TetraK and Cube with an higher porosity (i.e., 0.9 with respect to 0.8 of the random).

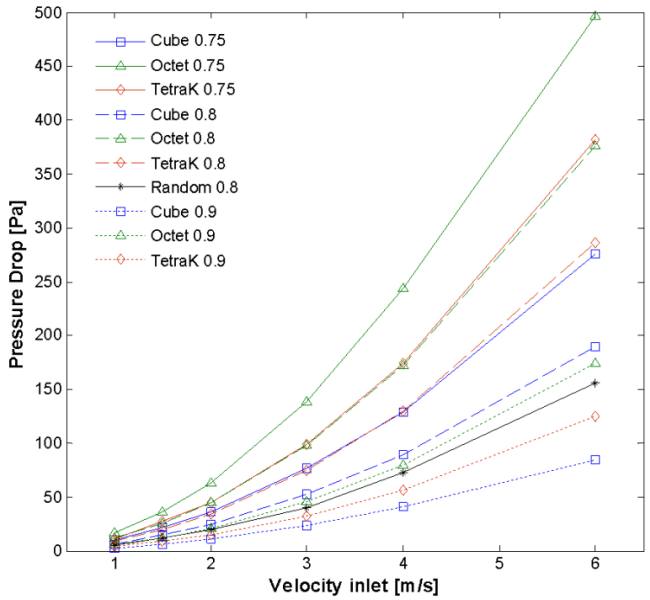

Figure 7 CFD results, pressure drop vs velocity inlet (For interpretation of the references to colour in this figure legend, the reader is referred to the web version of this article)

Heat Transfer coefficient

The cellular convective heat transfer coefficient was evaluated as:

$$h = \frac{\dot{Q}}{A \cdot \Delta T} = \frac{\dot{q}}{\Delta T} \qquad (4)$$

where Q is the heat flux across the foam surface, A is the cells surface and ΔT is defined as:

$$\Delta T = T_{wall} - \left(\frac{T_{inlet} + T_{outlet}}{2} \right) \qquad (5)$$

The calculated convective heat transfer coefficients as function of the air velocity are shown in Figure 8. As expected, h increases with air velocity, but it can be noticed that a precise separation among performance of cube, on one hand and TetraK and Octet on the other hand, exists. The two groups of results are sharply separated by the line corresponding to random foams. Cube lattice performance is poor for all porosities, whereas the best performance is shown by the Octet with 0.9 porosity for the entire range of velocity studied.

Nusselt Number

To describe the foams heat exchange performance in terms of nondimensional numbers, h was used to evaluate the Nusselt number:

$$Nu = \frac{h \cdot L_c}{\lambda_{fluid}} \qquad (6$$

where Lc is the characteristic length (in this case equal to D_h), λ_{fluid} is the air thermal conductivity (λ_{fluid} = 0.0242 [W/m-K]). Nusselt number trends for lattices and random foam vs Reynolds number are shown in Figure 9. This Figure shows that a sharp performance separation still exists between TetraK and Cube lattices, in fact, for all porosity values, the former are above the random foam line, whereas the latter are below it. Figures 10 shows also that, for a given porosity value, the Octed has a Nusselt number lower than the TetraK. In comparison with heat transfer coefficient results, being the fluid thermal conductivity constant, the Nu different behavior is played by the cell hydraulic diameter, which is favorable to TetraK as also shown by the pressure drop results.

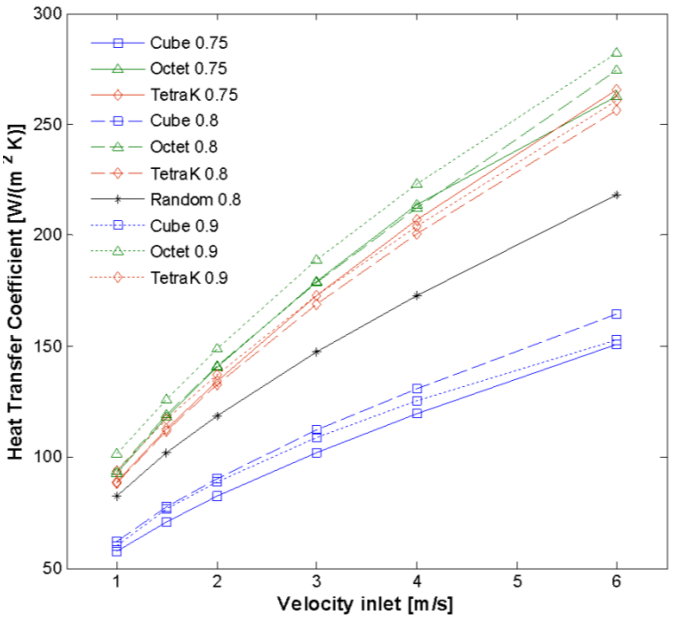

Figure 8 CFD results, convective heat transfer coefficient vs velocity inlet (For interpretation of the references to colour in this figure legend, the reader is referred to the web version of this article)

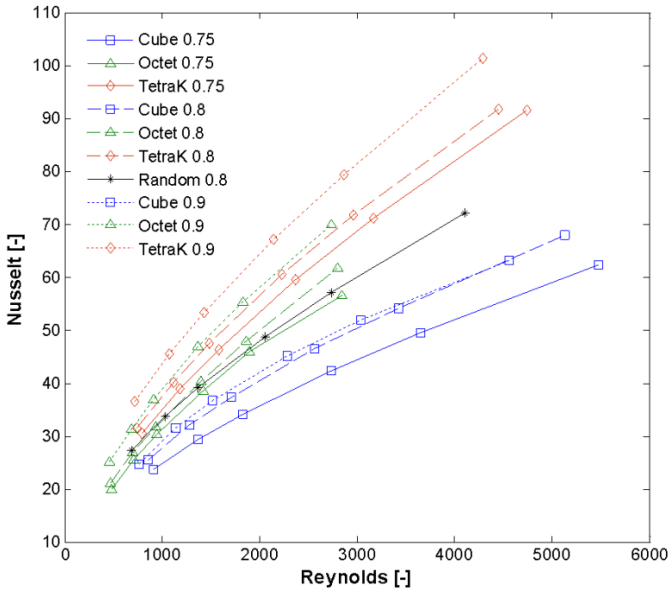

Figure 9 CFD results, Nusselt vs Reynolds (For interpretation of the references to colour in this figure legend, the reader is referred to the web version of this article)

Nusselt Number Correlations

From the results obtained, the lattice and random foam Nusselt number could be expressed with the following correlation:

$$Nu = a \cdot Re^{b} \cdot Pr \qquad (7)$$

where a and b are constant factors, specific for each porous media and porosity value. Re is the Reynolds number and Pr is the Prandtl number. In this work, being the fluid properties kept constant, the Prandtl number is identical in all test cases. Values of parameters a and b are reported in Table 2.

Table 2: Nusselt number correlations for lattices

	Geometries					
	Octet modified		Cube		TetraK	
	a	b	a	b	a	b
ε = 0.75	0.5419	0.783ε	0.6078	0.716ε	0.5067	0.818ε
ε = 0.80	0.5343	0.747ε	0.6604	0.677ε	0.6171	0.744ε
ε = 0.90	0.7430	0.637ε	0.8117	0.576ε	0.8530	0.570ε

From the correlations reported in Table 1 it can be noticed that, when varying the porosity, the increment of the exponent b is similar for all lattice geometries. This increment is about 0.94 passing from a porosity of 0.75 to 0.8 and it is about 0.85 for the passage from 0.8 to 0.9.

CONCLUSIONS

In this work, the heat exchanger performance of cellular materials, both random (i.e. foams) and regular (i.e. lattices) was studied via three-dimensional thermo fluid dynamics simulations. The CFD study was performed using the commercial CFD package ANSYS Fluent.

One random foam and three regular lattices, Cube, Octet and Tetrakaidecahedron were tested. The former had a porosity of 0.8, whereas the latter had porosities varying from 0.75 to 0.9.

Pressure drop results showed that, for the range of air velocities explored, random foam performance is outstanding with respect to porous media with same porosity. Better performance is offered only by TetraK and Cube with an higher porosity (i.e., 0.9 with respect to 0.8 of the random). Pressure drop increases when porosity reduces and the worst performance was obtained by the Octet with porosity 0.75.

For the convective heat exchange coefficient a precise separation among performance of cube (lowest), on one hand and Tetrak and Octet (highest) on the other hand, exists. Random foam performance stays in between. The best performance is shown by the Octet with 0.9 porosity, whereas Cube lattice performance is the lowest for all porosity values explored.

Nusselt number simple correlations were defined for all cellular samples. Nusselt number results showed the TetraK be the best performer for each given porosity and confirmed the cube be the worst one.

REFERENCES

[1] M. Scheffler, P. Colombo, Cellular Ceramics: Structure, Manufacturing, Properties and Applications, WILEY-VCH Verlag, 2005.

[2] Schwartzwalder, K. and Somers, A.V. Method of making porous ceramics articles, City, 1963

[3] A. Ortona, C. D'Angelo, S. Gianella, D. Gaia, "Cellular ceramics produced by rapid prototyping and replication", Materials Letters, Vol. 80, 1 August 2012, 95–98

[4] S. Pusterla, M. C. Barbato, A. Ortona, C. D'Angelo, "Numerical study of cell morphology effects on convective heat transfer in reticulated ceramics", Vol. 55, Issues 25–26, December 2012, Pages 7902–7910

[5] Z. Wu, C. Caliot, G. Flamant, Z. Wang, "Numerical simulation of convective heat transfer between air flow an ceramic foams to optimize volumetric solar air receiver performances", International Journal of Heat Mass Transfer, Vol. 54 (2011), 1527-1537

[6] VSG, Burlington, MA, USA

[7] Ansys Inc. Canonsburg, Pennsylvania, USA.

[8] Altair, MI, USA.

[9] H.K. Versteeg, W. Malalasekera, An introduction to Computational Fluid Dynamics. The Finite Volume Method. Longman Scientific and Technical, Harlow, 1995

[10] M.F. Ashby, A.G. Evans, N.A. Fleck, L.J. Gibson, J.W. Hutchinson, H.N.G. Wadley, "Metal foam – A Design Guide", Butterworth-Heinemann, Boston, 2000

[11] M. Ashby, Hybrid materials to expand the boundaries of material-property space, J. Am. Ceram. Soc. 94 (2011) S3–S14.